Numerical Computational of Fluid Flow through a Sclera Buckling

Lim Yeou Jiann [1, a)], Zuhaila Ismail [1, b)], Sharidan Shafie [1, c)] and Alistair Fitt [2, d)]

[1] *Department of Mathematical Sciences, Faculty of Science, Universiti Teknologi Malaysia, 81310 UTM Johor Bahru, Johor Darul Takzim, Malaysia.*

[2] *Faculty of Technology, Design and Environment, Oxford Brookes University Headington Campus, Gipsy Lane, Oxford, OX3 OBP, United Kingdom.*

[c)] Corresponding author: sharidan@utm.my
[a)] jiann8807@hotmail.com,
[b)] zuhaila@utm.my,
[d)] afitt@brookes.ac.uk

Abstract. In this paper, the implementation of the finite element analysis on the investigation of a phenomenon of fluid flow through a detached retina with sclera buckling treatment is elaborated. To analyze the fluid flow, a paradigm mathematical model is developed. The velocity profile and pressure distribution are simulated. Based on the analysis, it is found that the scale effects which arises from difference in size of the sclera buckling do affects the velocity profile in the human eye. It is important to comprehend the effect of the sclera buckling on the dynamics of the vitreous humour in order to improve the sclera buckling treatment on curing retinal detachment.

Keywords: Retinal Detachment, Sclera Buckling, and Finite Element Analysis.
PACS: 47.11.Fg

INTRODUCTION

The vitreous is a transparent gel with viscoelastic rheological properties. However, liquefaction of the vitreous humour happen due to the ageing [1, 2]. Rhegmatogeneous retinal detachment, RRD may occurs when the liquefied vitreous humour flow through a tear or break on the retina into the subspace between the retina and the retinal pigment epithelium, then pushed the retina away from the choroid [1-5]. Scleral buckling (SB) is always suggested to treat uncomplicated RRD [3, 6]. SB procedures for repair of retinal detachment without release the subretinal fluid have become increasingly popular. Serious intraocular complication associated with the choroidal perforation for drainage of subretinal fluid, including subretinal hemorrhage and retinal incarceration can be avoided by applying this technique [7-9]. However, some specific problems such as giant retinal tears, preretinal retraction, closure of the central retina artery after buckling, possible scleral rupture in staphylomatous eyes, and the localization of retinal tears on high bullous detachment, are not recommended for SB without drainage [10]. SB is normally made either by semi-hard plastic, silicone sponge, rubber, or donor sclera [2]. In order to treat the RRD, ophthalmologist will sew the SB within the sclera where the detached retina exist. Therefore, the traction on the retina will be relieved and then the retinal tear will settle against the wall of the eye. Consequently, enable the chorioretinal adhesions to be formed and seal the retinal break [2, 3]. Encircling scleral buckling surgery is named, if a silicone band or buckle is placed around the eyeball. On the other hand, if segmental silicon is placed, it is known as segmental scleral buckling surgery [3]. The popularity of SB surgery has gained attentions of many researchers [7, 11-15]. The tomographic features of the neurosensory retina after successful RRD surgery were investigated by Hagimura et al. [12]. Foveal retinal detachment may persist after successful scleral buckling surgery in eyes which

delay the visual acuity improvement. Two methods, which are Pars Plana Vitrectomy (PPV) with PPV and SB (PPV/SB), for repair of RRD were compared by Mehta et al. [13]. The authors conclude that PPV/SB had smaller risk for retinal redetachment when compared to PPV for repair of phakic RRD.

Besides that, the SB that suture on the sclera will indent the wall of the eye and frequently, the indentation beneath the hole or tear on the retina do not against the back of the eye. Thus, the liquefied vitreous humour is still free to flow into the subspace between the detached retinal and choroid. However, the attachment of the retina still happen. The mechanism of the retina attaches to the choroid after the placement of the SB is equivocally. Several researches [7, 14, 15] have attempted to explain this phenomena either numerically, analytically or experimentally. Hammer [7] had showed analytically for the case of stationary retina, a force was created by the fluid flow from the vitreous cavity through the hole toward the sub retinal space for the attachment of the retinal. A simplified experimental model had been computed by Clemens et al. [15] to analyses this problem. Clemens and associated had considered the movement of the eye, such as saccadic eye movement or rapid eye movement, to the fluid flow in the vitreous cavity. Foster et al. [14] commented that the fluid movement which cause the detachment are also responsible for the reattachment of the retina when the hole is still elevated and had opinion that the speed of fluid absorption by the pigment epithelium is not sufficient to explain the phenomena. Recently Foster et.al. [14] have extended the research done by Clement et.al. [15] to obtain a qualitative and quantitative analysis of the phenomena occurring using the COMSOL Multiphysics. In particular, they found that rapid eye movements facilitate more rapid retinal reattachment.

Motivated by research mentioned above, we intend to extend the work done by Foster et.al. [14] in order to understand the effect of the SB surgery on the movement of liquefies vitreous humour to the retinal attachment especially when the size of the SB is changed. Finite element methods have been proposed by the Clement et.al. [15] and Foster et.al. [14]. Some researchers [16-20] have used the method to solve the problem in fluid mechanics and found out that the method work efficiently. Finite element method is easily applied to objects with complex geometry and having mixed boundary conditions and the objects may composed of several different materials in its medium [18-22]. Therefore, we advocate to solve the problem numerically by using finite element method. However, to the best of authors' knowledge, the detail of the application of the finite element analysis to solve this problem is not adequately provided. Ours long term goal is to use computer simulation to explore the fluid mechanics involved in different form of RRD and SB and to predict the response to possible treatment. As a step toward this final objective, the immediate aim herein is to elaborate the procedures of applying the finite element method on analyzing the fluid movement toward the SB and develop a computer model to be able to account for the mechanical.

MATHEMATICAL FORMULATION

The flow of liquefied vitreous humour through the detached retina and sclera buckling is studied by using a paradigm mathematical model. Since the curvature of the eye is not perceptible from the detached retina, thus the choroid is assumed as a plane wall [1, 3, 23]. The liquefied vitreous humour have properties very similar to water [1-3, 23], therefore, we treat the vitreous humour as a Newtonian fluid. A steady two-dimensional flow of an incompressible Newtonian fluid with constant viscosity, μ and density, ρ pass through a channel as shown in Fig. 1, where $y = f(x)$ and $y = H$ are fixed walls in a Cartesian coordinate system is considered in this research. The upper choroid wall and the deformation shape of the lower choroid wall by the sclera buckling are represented by $y=H$ and $y=f(x)$ respectively.

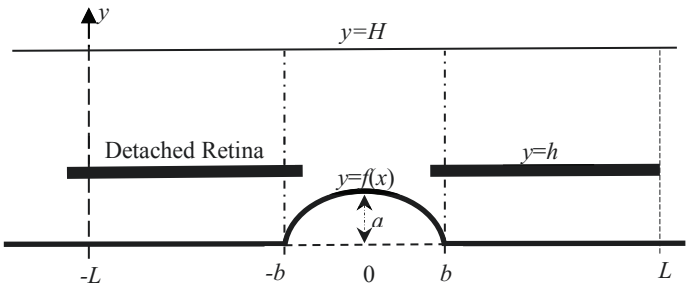

FIGURE 1. Schematic diagram of the detached retina and sclera bucking

The retina detachment is represented by $y=h$. Then, u, v and p will be used to illustrate the velocities in the x and y directions and pressure respectively. We assume, for reality, the height of the detached retina, is h = 0.1mm and the length of the detached retina is L= 1.0mm. Following [3], a normal human eye has diameter, H = 25mm and the vitreous humour has a typical velocity of $U \sim 2.1\times10-5\text{ms}^{-1}$ and the kinematic viscosity of the liquefied vitreous humour is $v = \mu/\rho \sim 0.9\times10\text{-}6\text{m}^2\text{s}^{-1}$. a is the size of the SB. The equations that govern the flow of liquefied vitreous humour toward to the retinal detachment and SB are:

$$-\frac{\partial p}{\partial x}+\nu\left(\frac{\partial^2 u}{\partial y^2}+\frac{\partial^2 u}{\partial x^2}\right)=\rho\left(u\frac{\partial u}{\partial x}+v\frac{\partial u}{\partial y}\right),\quad -\frac{\partial p}{\partial y}+\nu\left(\frac{\partial^2 v}{\partial y^2}+\frac{\partial^2 v}{\partial x^2}\right)=\rho\left(u\frac{\partial v}{\partial x}+v\frac{\partial v}{\partial y}\right),\quad \frac{\partial u}{\partial x}+\frac{\partial v}{\partial y}=0. \tag{1}$$

The governing equations given in (1) will be solved subjected to the no slip conditions on $y = f(x)$, $y=h$ and $y=H$. The boundary conditions for the velocity in each region are:

$$u\left(x,f\left(x\right)\right)=v\left(x,f\left(x\right)\right)=u\left(x,h\right)=v\left(x,h\right)=u\left(x,H\right)=v\left(x,H\right)=0. \tag{2}$$

FINITE ELEMENT ANALYSIS

In order to solve Eq. (1) subject to the boundary conditions (2) by using finite element methods, we discretized the domain as shown in Fig. 1 into finite number of subdomains. Each subdomains are called as finite element. In this research, Taylor-Hood elements on triangles were used to construct the domain. In fact, Taylor-Hood elements have satisfied the discrete inf-sup condition which guarantee the existence and stability for the Eq. (1) subjected to the boundary conditions (2) (see [20] for detail.). Then, the weighted residual methods [18, 19, 21, 22] was applied to Eq. (1) over the element. Multiplying Eq. (1) by the arbitrary weight functions, ϕ_1 and ϕ_2, and integrating over the domain, we obtain

$$\int_{A_e}\phi_1\begin{pmatrix}-\frac{\partial p_k^*}{\partial x}+\nu\left(\frac{\partial^2 u^*}{\partial y^2}+\frac{\partial^2 u^*}{\partial x^2}\right)-\rho\left(u^*\frac{\partial u^*}{\partial x}+v^*\frac{\partial u^*}{\partial y}\right)\\ -\frac{\partial p^*}{\partial y}+\nu\left(\frac{\partial^2 v^*}{\partial y^2}+\frac{\partial^2 v^*}{\partial x^2}\right)-\rho\left(u^*\frac{\partial v^*}{\partial x}+v^*\frac{\partial v^*}{\partial y}\right)\end{pmatrix}dA=\begin{pmatrix}0\\0\end{pmatrix},\quad \int_{A_e}\phi_2\left(\frac{\partial u^*}{\partial x}+\frac{\partial v^*}{\partial y}\right)dA=0. \tag{3}$$

u^*, v^* and p^* are the approximation solutions for the velocity components and pressure respectively and A_e is the surface integral of a finite element. Now let

$$u\cong u^*=\sum_{i=1}^{6}u_i\psi_i,\quad v\cong v^*=\sum_{i=1}^{6}v_i\psi_i \text{ and } p\cong p^*=\sum_{j=1}^{3}p_j\varphi_j. \tag{4}$$

ψ_i and φ_j are called the shape functions (see [18, 19, 21, 22]) for the velocity and pressure respectively, u_i, v_i, and p_j are the local values of the velocity components at a specific node, i, and the pressure at a specific node, j, in the element. Galerkin finite element methods was applied in this research to compute the numerical solutions, therefore, we choose $\phi_1=\psi_i$, and $\phi_2=\varphi_j$. Then, Eq. (4) is substituted into Eq. (3) and the integration by part technique is applied to obtain the weak form of the governing equation, given as

$$\int_{A_e}\begin{Bmatrix} -\dfrac{\partial\psi_i}{\partial x}\sum_{j=1}^{3}p_j\varphi_j+\nu\left(\dfrac{\partial\psi_i}{\partial y}\dfrac{\partial\sum_{i=1}^{6}u_i\psi_i}{\partial y}+\dfrac{\partial\psi_i}{\partial x}\dfrac{\partial\sum_{i=1}^{6}u_i\psi_i}{\partial x}\right)-\rho\psi_i\left(\sum_{i=1}^{6}u_i\psi_i\dfrac{\partial\sum_{i=1}^{6}u_i\psi_i}{\partial x}+\sum_{i=1}^{n}v_i\psi_i\dfrac{\partial\sum_{i=1}^{6}u_i\psi_i}{\partial y}\right) \\ -\dfrac{\partial\psi_i}{\partial y}\sum_{j=1}^{3}p_j\varphi_j+\nu\left(\dfrac{\partial\psi_i}{\partial y}\dfrac{\partial\sum_{i=1}^{6}v_i\psi_i}{\partial y}+\dfrac{\partial\psi_i}{\partial x}\dfrac{\partial^2\sum_{i=1}^{6}v_i\psi_i}{\partial x^2}\right)-\rho\psi_i\left(\sum_{i=1}^{6}u_i\psi_i\dfrac{\partial\sum_{i=1}^{6}v_i\psi_i}{\partial x}+\sum_{i=1}^{n}v_i\psi_i\dfrac{\partial\sum_{i=1}^{6}v_i\psi_i}{\partial y}\right)\end{Bmatrix}dA$$

$$=\oint_{l_e}\begin{Bmatrix} -p^*n_x+\mu\left(\dfrac{\partial u^*}{\partial x}\hat{n}_x+\dfrac{\partial u^*}{\partial y}\hat{n}_y\right) \\ -p^*n_y+\mu\left(\dfrac{\partial v^*}{\partial x}\hat{n}_x+\dfrac{\partial v^*}{\partial y}\hat{n}_y\right)\end{Bmatrix}dl, \tag{5a}$$

$$\int_{A_e}\varphi_j\left(\frac{\partial\sum_{i=1}^{6}u_i\psi_i}{\partial x}+\frac{\partial\sum_{i=1}^{6}v_i\psi_i}{\partial y}\right)dA=0, \tag{5b}$$

l_e is the line integral of a finite element. Eq. (5a)-(5b) can be illustrated in a sophisticated form which is in form of matrix. Therefore, we have

$$\begin{bmatrix} K & -C \\ -C^T & \{0\}\end{bmatrix}\begin{bmatrix}\{u\}^T \\ \{p\}^T\end{bmatrix}=\begin{bmatrix} I \\ \{0\}\end{bmatrix} \tag{6}$$

where,

$$K=-K_1+K_2+K_3,$$

$$K_1=\int_{A_e}\rho[N]^T[N]\left(\{u^e\}\frac{\partial[N]}{\partial x}+\{v^e\}\frac{\partial[N]}{\partial y}\right)dA,\quad K_2=\int_{A_e}\nu\frac{\partial[N]}{\partial x}\frac{\partial[N]^T}{\partial x}dA,\quad K_3=\int_{A_e}\nu\frac{\partial[N]}{\partial y}\frac{\partial[N]^T}{\partial y}dA,$$

$$[N]=\begin{pmatrix}\psi_1 & 0 & \psi_2 & 0 & \cdots & \psi_6 & 0\\ 0 & \psi_1 & 0 & \psi_2 & \cdots & 0 & \psi_6\end{pmatrix},\quad \{u^e\}=(u_1\quad u_2\quad\cdots\quad u_6),\quad \{v^e\}=(v_1\quad v_2\quad\cdots\quad v_6),$$

$$C=\int_{A_e}\begin{pmatrix}\dfrac{\partial\psi_1}{\partial x} & \dfrac{\partial\psi_1}{\partial y} & \cdots & \dfrac{\partial\psi_6}{\partial x} & \dfrac{\partial\psi_6}{\partial y}\end{pmatrix}^T(\varphi_1\quad\varphi_2\quad\varphi_3)\,dA,$$

$$\{u\}=(u_1\quad v_1\quad u_2\quad v_2\quad\cdots\quad u_6\quad v_6),\quad \{p\}=(p_1\quad p_2\quad p_3),$$

$$I=\oint_{l_e}[N]^T\begin{pmatrix}-p^*n_x+\mu\left(\dfrac{\partial u^*}{\partial x}\hat{n}_x+\dfrac{\partial u^*}{\partial y}\hat{n}_y\right) & -p^*n_y+\mu\left(\dfrac{\partial y^*}{\partial x}\hat{n}_x+\dfrac{\partial v^*}{\partial y}\hat{n}_y\right)\end{pmatrix}^T dl.$$

Eq. (6) is the element matrices and vectors for every element. To determine the velocity profile and the pressure distribution of the fluid flow toward the SB, the system matrix and vector are obtained by assembly the element matrices and vectors. Then, the system matrix and vector equation is solved by subjected to the given boundary conditions, Eq. (2) to obtain the essential variables.

RESULTS AND DISCUSSION

A Matlab coding was developed to compute the numerical results and a personal computer with a processor speed of 2.30 GHz and a RAM of 8GB was used to run all the computation in the study. A mesh test was conducted to show that the results do not affected by the number of elements and nodes (see Figs. 2(a)-2(c)). Observation from

these figures, we acknowledged that the numerical results determined by using total number of elements from 2959 to 6031 and nodes from 1754 to 3364 have the same output. Therefore, we hold the view that the number of elements and nodes will not affect the results. Comsol Multiphysics software was also used to simulate the fluid flow, 5064 elements were used to compute the result and the result (see Fig. 2(d)) is concurrent to the results that we have computed (see Figs. 2(a)-2(c)). Experimental results conducted by Clemens et.al. [15] were compared with the computed numerical output in this research for validation. Clemens et al. [15] showed that the subretinal fluid was moving out, which driven by the movement of the eye (i.e. saccadic motion, rapid eye motion), into the model's vitreous through the hole when a buckle was positioned under the hole. The computation simulation (see Fig. 3(d)) has showed a great agreement with the description of fluid flow that observed experimentally by Clemens et al. [15]. We observed from Fig. 3(d) that the fluid flows out of the subretinal space into the vitreous cavity through the hole whereas there is no fluid flows out of the subretinal space through the hole (see Fig. 3(a)) when the buckle was not sutured. The great agreement between the present results with the previous obtained solutions and also the computational output by Comsol software has enhanced our confidence to the results determined in this research. 5500 to 6000 elements were used to conduct the results shown in Fig. 3. The figures illustrated that the increasing of value *a* from 0 to 0.018 have make an anecdotal change to the behaviour of the fluid. The results show that the scale effects which arises from difference in size of the SB do effect the fluid behaviour in the human eye. Different size of the SB will cause the vitreous humour behave differently. In fact, the pigment epithelium will absorb the subretinal fluid but we agreed with Clemens et al. [14] that the speed of fluid absorption is not sufficient to explain the rapid reducing of subretinal fluid and the reattachment of the retina when a retinal hole is still elevated. Therefore, we concluded that when a proper size SB is used, the subretinal fluid will flow out of the subretinal space faster and then induced the detached retina to attach itself and may reduce the duration of the recovery from the retinal detachment. Further research is needed to fully understand the real mechanism of the vitreous humour under the effect of SB.

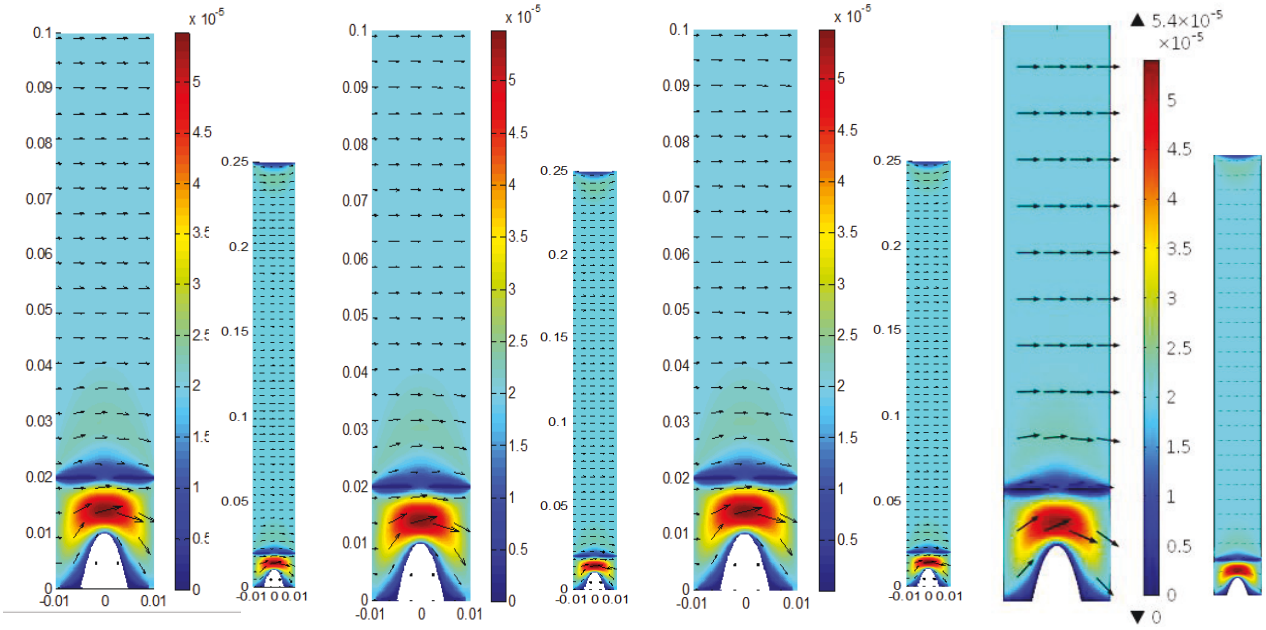

(a) Elements = 2959 and Nodes =1754.

(b) Elements = 4635 and Nodes =2656.

(c) Elements = 6031 and Nodes =3364.

(d) Comsol Result with Elements= 5064.

FIGURE 2. Mesh test.

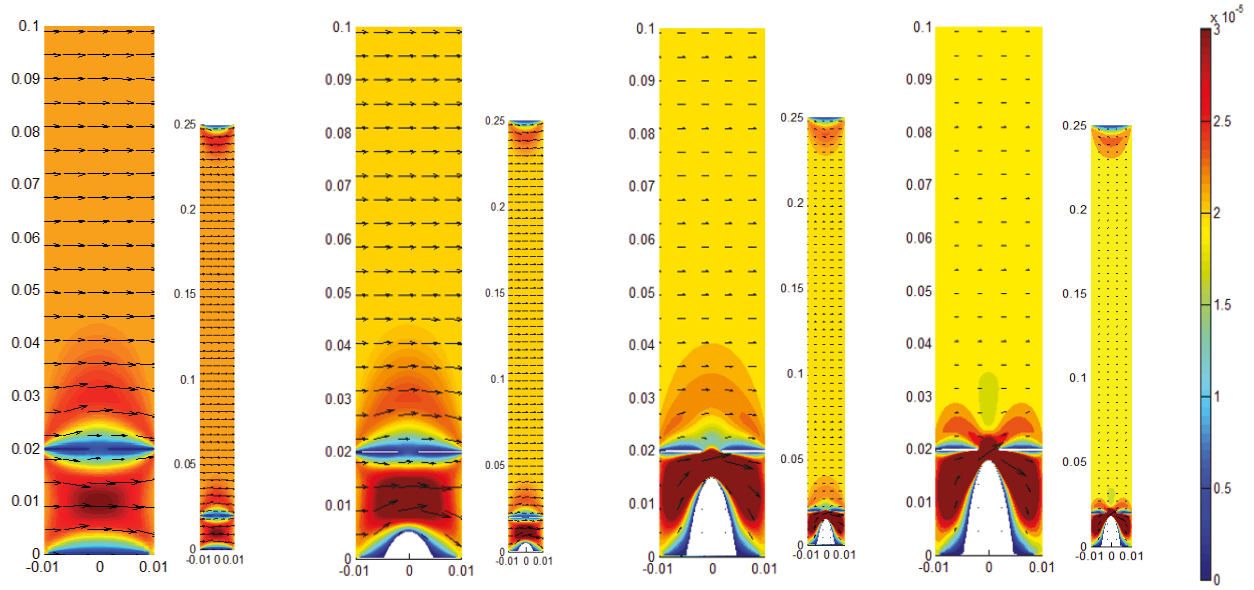

(a) $a = 0$. (b) $a = 0.005$. (c) $a = 0.015$ (d) $a = 0.018$

FIGURE 3. The scale effect developed by difference size of the SB, a, to the velocity profile of the liquefied vitreous humour.

CONCLUSION

The behaviour of the liquefied vitreous humour in the subretinal space under the effect of SB have been analyzed. Some figures are plotted to show the behaviour of the fluid under different size of SB. Some interesting finding of the study can be concluded as follows:

1. The velocity of the liquefied vitreous humour is effected by the size of the SB.
2. The subretinal fluid is flow out of the subretinal space through the tear or hole when a proper SB are used in the treatment of RRD which will enhance the period of reattachment of the retinal.
3. The computation model and the Matlab coding that developed in this study can be used to analyze the fluid flow in human eye under effect of SB and also suggested to be applied to investigate a move advance research in the future.

In our opinion, for future research we should consider the fluid flow into the real shape of the vitreous chamber and the visco-elastic behavior of the vitreous in physiological conditions.

ACKNOWLEDGMENTS

The authors would like to acknowledge KPT (MyBrain), MoHE and Research Management Centre – UTM for the financial support through vote numbers 06H67, 4F255, 08H53, 4F632 and 4F538 for this research.

REFERENCES

1. F. Alistair, D. Rosemary, J. Oliver, M. Nigel, M. Dmitri, N. Shailesh, O. Raffaella, S. Jennifer and S. Andrew, 2004.
2. A. B. Daniel and C. P. Wilkinson, *Retinal Detachment : Priniciples and Practice: Priniciples and Practice*.Oxford University Press, USA, 2009.
3. I. Zuhaila, Ph.D. Thesis, University of Southampton, 2013.
4. P. Riordan-Eva and E. Cunningham, *Vaughan & Asbury's General Ophthalmology, 18th Edition*.McGraw-Hill Education, 2011.
5. B. Cook, G. P. Lewis, S. K. Fisher and R. Adler, Invest. Ophth. Vis. Sci. **36** (6), 990-996 (1995).
6. A. Sodhi, L. S. Leung, D. V. Do, E. W. Gower, O. D. Schein and J. T. Handa, Survey of ophthalmology **53** (1), 50-67 (2008).

7. M. E. Hammer, Docum. Ophthal. Proc. Ser. **25**, 61-75 (1981).
8. A. H. Chignell, American journal of ophthalmology. **77** (1), 1-5 (1974).
9. T. Daniel and M. D. Weidenthal, American journal of ophthalmology. **63** (1), 108-112 (1967).
10. R. Patrick and M. D. O'Connor, American journal of ophthalmology. **76** (1), 30-34 (1973).
11. C. M. Greven, A. B. Wall and M. M. Slusher, Am J Ophthalmol **128** (5), 618-620 (1999).
12. N. Hagimura, T. Iida, K. Suto and S. Kishi, Am J Ophthalmol **133** (4), 516-520 (2002).
13. S. Mehta, K. J. Blinder, G. K. Shah and M. G. Grand, Canadian journal of ophthalmology. Journal canadien d'ophtalmologie **46** (3), 237-241 (2011).
14. W. J. Foster, N. Dowla, S. Y. Joshi and M. Nikolaou, Graefes Arch Clin Exp Ophthalmol **248** (1), 31-36 (2010).
15. S. Clemens, P. Kroll, E. Stein, W. Wagner and P. Wriggers, Graefes Arch Clin Exp Ophthalmol **225**, 16-18 (1997).
16. M. Sajid, R. Mahmood and T. Hayat, Comput. Math. Appl. **56** (5), 1236-1244 (2008).
17. R. Mahmood, M. Sajid and A. Nadeem, Adv. Stud. Theor. Phys. **5** (3), 107-120 (2011).
18. J. N. Reddy and D. K. Gartling, *The Finite Element Method in Heat Transfer and Fluid Dynamics, Third Edition*.Taylor & Francis, 2010.
19. O. C. Zienkiewicz, R. L. Taylor and P. Nithiarasu, *The Finite Element Method for Fluid Dynamics*.Elsevier Science, 2013.
20. L. Jichun and C. Yi-Tung, *Computational Partial Differential Equations Using MATLAB*.Taylor & Francis Group, Boca Raton, 2008.
21. J. N. Reddy, *An Introduction to the Finite Element Method*.McGraw-Hill Education, USA, 2006.
22. A. J. Davies, *The Finite Element Method*, 2 ed.Oxford University Press, New York, 2011.
23. G. Gonzalez and F. Alistair, in *Mathematics Today* (2003).